Wang *et al. Geosci. Lett. (2016) 3:34*
DOI 10.1186/s40562-016-0066-z

Geoscience Letters

REVIEW Open Access

A trio-interaction theory for Madden–Julian oscillation

Bin Wang[1,2*], Fei Liu[1] and Guosen Chen[1,2]

Abstract

The Madden–Julian oscillation (MJO) is the dominant mode of tropical atmospheric intraseasonal variability and a primary source of predictability for global sub-seasonal prediction. Understanding the origin and perpetuation of the MJO has eluded scientists for decades. The present paper starts with a brief review of progresses in theoretical studies of the MJO and a discussion of the essential MJO characteristics that a theory should explain. A general theoretical model framework is then described in an attempt to integrate the major existing theoretical models: the frictionally coupled Kelvin–Rossby wave, the moisture mode, the frictionally coupled dynamic moisture mode, the MJO skeleton, and the gravity wave interference, which are shown to be special cases of the general MJO model. The last part of the present paper focuses on a special form of trio-interaction theory in terms of the general model with a simplified Betts–Miller (B-M) cumulus parameterization scheme. This trio-interaction theory extends the Matsuno–Gill theory by incorporating a trio-interaction among convection, moisture, and wave-boundary layer (BL) dynamics. The model is shown to produce robust large-scale characteristics of the observed MJO, including the coupled Kelvin–Rossby wave structure, slow eastward propagation (~5 m/s) over warm pool, the planetary (zonal) scale circulation, the BL low-pressure and moisture convergence preceding major convection, and amplification/decay over warm/cold sea surface temperature (SST) regions. The BL moisture convergence feedback plays a central role in coupling equatorial Kelvin and Rossby waves with convective heating, selecting a preferred eastward propagation, and generating instability. The moisture feedback can enhance Rossby wave component, thereby substantially slowing down eastward propagation. With the trio-interaction theory, a number of fundamental issues of MJO dynamics are addressed: why the MJO possesses a mixed Kelvin–Rossby wave structure and how the Kelvin and Rossby waves, which propagate in opposite directions, could couple together with convection and select eastward propagation; what makes the MJO move eastward slowly in the eastern hemisphere, resulting in the 30–60-day periodicity; why MJO amplifies over the warm pool ocean and decays rapidly across the dateline. Limitation and ramifications of the model results to general circulation modeling of MJO are discussed.

Keywords: Madden–Julian oscillation, MJO theory, Tropical wave dynamics, Convectively coupled equatorial waves, Trio-interaction theory for MJO, Moisture mode, Dynamic moisture mode

Background

Madden and Julian (1971) discovered a 40–50-day oscillation in tropospheric zonal winds at the equatorial central Pacific. This local 40–50-day oscillation is later understood as associated with an equatorial planetary-scale circulation system coupled with large-scale convection that moves eastward slowly with a speed of about 5 m/s in the eastern hemisphere (Madden and Julian 1971; Nakazawa 1988). This phenomenon is named as Madden–Julian oscillation (MJO). In general, tropical atmospheric motion exhibits a significant energy peak on a broad range of 2–8 weeks, which is often referred to as tropical intraseasonal variability. The MJO is the dominant mode of tropical intraseasonal variability that bridges weather and climate variation.

Prediction of extreme weather events two-to-six weeks ahead (also called sub-seasonal prediction) has immense

*Correspondence: wangbin@hawaii.edu
[1] Earth System Modeling Center, Nanjing University of Information Science and Technology, Nanjing, China
Full list of author information is available at the end of the article

social–economic benefits for hazard prevention and risk management as well as economic planning. The physical basis for such sub-seasonal prediction is primarily rooted in the predictability of large-scale circulation associated with the MJO and the regulation of the MJO on extreme and high-impact weather events such as tropical storms, flooding, droughts, heavy snow storms, heat waves, cold surges, wild fires, hazes, tornado and hail days (Zhang 2013; Wang and Moon 2016). The MJO is considered as a major source of global predictability on the sub-seasonal timescale (Waliser 2012).

Dynamical MJO prediction has significantly advanced. The prediction skills for the first two leading modes have increased from 7 days during 1990s to about 25–30 days (ECMWF and GFDL models) during 2010s (Vitart 2014; Xiang et al. 2015). However, the models still have large room to reach potential predictability limit (Neena et al. 2014; Lee et al. 2015). Realistic simulation of MJO in many current general circulation models (GCMs) remains a great challenge (Jiang et al. 2015). Understanding the origin and perpetuation of the MJO has eluded scientists for decades. Further improvement of our understanding of the fundamental physics of the MJO is urgent and imperative. The present paper aims to promote theoretical understanding of the essential physics of MJO.

Review of progresses in theoretical understanding

A variety of theories and mechanisms have been proposed to explain various aspects of MJO over the past three decades. These theories are subjectively categorized as four groups of basic theories plus two groups of specific theories.

1. Convectively coupled Kelvin–Rossby wave theory. This theory is centered on interaction between convective heating, the low-frequency equatorial waves, and the boundary layer (BL) frictional moisture convergence, which integrated the mechanisms of the BL frictional moisture feedback (Wang 1988b; Wang and Chen 1989), non-linear wave-Conditional Instability of the Second Kind (CISK) (Lau and Peng 1987), and the evaporation-wind feedback (Emanuel 1987; Neelin et al. 1987; Wang 1988a). These mechanisms were later combined into a frictionally coupled moist Kelvin–Rossby wave theory (Wang and Rui 1990a; Wang and Li 1994; Kang et al. 2013). This theory explained why the observed MJO features a coupled Kelvin–Rossby wave structure (Rui and Wang 1990; Adames and Wallace 2014), why the low sea-level pressure and the BL moisture convergence lead the major convection in observations (Madden and Julian 1972; Hendon and Salby 1994; Jiang and al 2015), and why MJO moves eastward and can be unstable on planetary scales (Wang 1988b; Wang and Rui 1990a; Li and Zhou 2009). The role of frictional moisture feedback also implies potentially important roles of the shallow-congestus convection–BL circulation interaction in MJO dynamics as proposed by Johnson et al. (1999), Lin et al. (2004), and Kikuchi and Takayabu (2004). The weakness of the theory is the use of a diagnostic moisture equation and moisture feedback process is neglected. The resulting eastward propagation speed is 10–15 m/s, which is too fast for a warm sea surface temperature (SST) of 29 °C. As suggested by Moskowitz and Bretherton (2000), the damping magnitude of the BL friction may be too large in Wang and Rui (1990a).

2. The moisture mode theory. This theory regards the moisture (or moist static energy) as the first order important. It emphasizes moisture–convection feedback (Woolnough et al. 2001; Grabowski and Moncrieff 2004) and moisture transport (Maloney 2009; Maloney et al. 2010; Andersen and Kuang 2012; Hsu and Li 2012; Kim et al. 2014; Pritchard and Bretherton 2014; Liu and Wang 2016a, b). A simple empirical model was proposed (Sobel and Maloney 2012, 2013), which is further implemented by Adames and Kim (2016). The MJO instability mainly comes from the parameterized cloud-radiative feedback by choice of negative "effective gross moist stability". The eastward propagation is mainly driven by meridional advection of mean moisture by MJO winds, and the parametrized BL convergence effect. This theory produces an MJO mode that is dispersive with a westward group velocity. In this model, the only prognostic variable is moisture anomaly; the circulation is a passive Gill-like (Gill 1980) response. The generation of MJO available potential energy is neglected due to the diagnostic thermodynamic equation used. The numerical experiments of Pritchard and Yang (2016) showed that the horizontal advection of moist static energy is not significant to the eastward propagation of MJO-like mode, so the model may underestimate the feedbacks of wave dynamics on the MJO's propagation.

3. The frictionally coupled dynamic moisture mode theory. The convectively coupled Kelvin–Rossby wave theory captures the interaction between convection and wave-BL dynamics but neglects moisture feedback. On the other hand, the moisture mode theory captures the convection–moisture feedback but neglects the interaction between the convective heating and wave-BL dynamics. Combination of the above two types of theory results in the frictionally coupled dynamic moisture mode model (Wang and Chen 2016, Liu and Wang 2016b). This dynamic moisture model uses a simplified Betts–Miller (B-M) cumulus parameterization scheme to describe moisture feedback. The trio-interaction among convective heating, moisture, and wave-BL dynamics yields a frictionally coupled dynamic moisture wave

packet that resembles observed MJO closely. This theory will be further discussed in "The MJO simulated in the MJO trio-interaction model" section.

4. The multiscale interaction theory. The MJO convective complex consists of multiscale convective activity and motions (Nakazawa 1988). How these mesoscale and synoptic-scale motions interact and contribute to MJO dynamics has been a controversial issue. Many different schools of thinking have been proposed in this regard. Here, we introduce four types of models belonging to this category.

a. The MJO skeleton model. The effects of synoptic waves on MJO through upscale momentum, heat, and moisture transports are considered as a potential driver for MJO (Majda and Biello 2004; Biello and Majda 2005; Wang and Liu 2011; Liu et al. 2012; Liu and Wang 2012c, 2013b). The MJO skeleton model driven by synoptic wave activity ensemble (Majda and Biello 2004; Majda and Stechmann 2009) is a simplest model generalizing this idea. In the skeleton model, the tendency of planetary-scale wave envelope is linked to the low-level moisture anomaly, which is essentially a kind of convective heating parameterization. This parameterization and resulted quadrupole structure remain to be validated against observations (Chen and Wang 2016). The skeleton model can produce a slow eastward-propagating mode with a dispersion feature in which frequency is nearly independent of wavenumber. The model, however, yields neutral modes which can propagate either eastward or westward (Majda and Stechmann 2009). Liu and Wang (2012a) extended the original skeleton model by including BL frictional feedback. The resulting frictional skeleton mode becomes an unstable, planetary-scale, eastward-propagating mode, while the original westward-propagating mode is damped. The skeleton model is also extended to include stochasticity in synoptic and convective activities, reproducing the intermittency, growth and decay, seasonal variation, and vertical tilt of the MJO (Thual et al. 2014).

b. The MJO–synoptic wave interaction model. In this model, the effects of momentum, heat and moisture transports by synoptic-scale motions are parametrized in the governing equations for the MJO motion (Wang and Liu 2011; Liu et al. 2012; Liu and Wang 2012c, 2013b). This type of models allows for a two-way interaction between high-frequency waves (inertial-gravity waves, Kelvin waves) and MJO. The impacts of the upscale momentum, heat and moisture transports to MJO were found to depend on the relative locations of the synoptic disturbance with respect to the MJO convective center. The MJO is found to amplify when the moist Kelvin waves are located to the west of the MJO convective center, meanwhile the westward-propagating inertia–gravity waves could have a positive feedback on the MJO when they are located to the east of the MJO convective center (Wang and Liu 2011).

c. The multi-cloud model. The MJO has the so-called "self-similarity" cloud structure (Mapes et al. 2006; Kiladis et al. 2009). To understand the multi-cloud structure of the MJO, a multi-cloud model has been built by Khouider and Majda (2006, 2007). The key features are (a) systematic low-level moisture convergence with retained conservation of vertically integrated moist static energy, and (b) the use of three cumulus cloud types (congestus, stratiform, and deep convective) together with their differing vertical heating structures. This multi-cloud model successfully simulates the MJO analog of slow eastward propagation, "self-similarity" vertical structure and multiscale horizontal structure (Majda et al. 2007). The wavenumber 3 is most unstable and the instability comes from the second vertical baroclinic mode. This stratiform cloud–wave interaction or moisture stratiform–wave interaction mechanisms have also been found to support MJO growth in other works (Mapes 2000; Kuang 2008; Fu and Wang 2009; Seo and Wang 2010).

d. The gravity wave interference model. Motivated by the existence of relatively short-lived, eastward- and westward-moving disturbances within the MJO complex, the MJO has been thought as a wave packet—the interference pattern produced by a narrow frequency band of mixed Rossby-gravity (Yang and Ingersoll 2011) or inertia–gravity waves (Yang and Ingersoll 2013, 2014). In this model, the MJO is treated as a large-scale envelope of small-scale gravity waves triggered by individual convective cells. The eastward propagation arises from a zonal asymmetry in inertial-gravity waves, and the MJO planetary scale depends on a scaling factor of convective strength vs. gravity wave speed. This wave packet theory explains only a small fraction of the variance of the MJO in the outgoing longwave radiation (OLR) data.

In addition to the aforementioned basic MJO theories, there are other specific theories focusing on "higher order" characteristics, including the boreal summer intraseasonal oscillation (ISO) theory and atmosphere–ocean interaction theory.

5. Theories for the boreal summer ISO (BSISO). The BSISO has characteristics distinguished from the MJO, which include (a) northward propagation, (b) formation of the northwest–southeast-tilted precipitation band, and (c) the shift of variability center to off-equatorial monsoon regions. Wang and Xie (1997) established a theory for the BSISO, which attributed the formation of the northwest–southeast-tilted precipitation band to emanation of the Rossby waves from the decaying equatorial MJO mode over the maritime continent and near the dateline. They also attributed the northward propagation to the effects

of the easterly vertical wind shears (easterly increase with height) in the monsoon regions. They showed that the basic state-specific humidity distribution and monsoon easterly vertical shear together shifts the centers of ISO variance to Northern Hemisphere summer monsoon regions. To explain northward propagation of the BSISO, several other mechanisms were also proposed, including the land surface heat fluxes (Webster and Holton 1982), the interaction between convection and moist stability (Gyoswami and Shukla 1984), the interaction between baroclinic and barotropic vorticity forced by vertical wind shear (Wang and Xie 1997; Jiang et al. 2004; Drbohlav and Wang 2005), the air–sea interaction (Kemball-Cook and Wang 2001; Fu and Wang 2004), the convective momentum transport-induced barotropic vorticity (Kang et al. 2010; Liu et al. 2015), the beta drift (Boos and Kuang 2010), and the BL moisture advection and the vertical wind shear-induced barotropic vorticity effect (DeMott et al. 2013).

6. The atmosphere–ocean interaction theory. The atmosphere–ocean interaction has been shown to play a role in sustaining the MJO (Flatau et al. 1997; Wang and Xie 1998; Wang and Zhang 2002; Fu and Wang 2004). The linear atmosphere–ocean interaction theory proposed by Wang and Xie (1998) and Liu and Wang (2013a) has demonstrated that the air–sea interaction under mean westerly winds is conducive to unstable, eastward-propagating planetary-scale waves on intraseasonal timescale. Although the cloud–shortwave radiation–SST feedback can destabilize both eastward and westward modes, the air–sea feedback associated with the evaporation and oceanic entrainment favors planetary-scale eastward-propagating modes. Over the western hemisphere where easterly background winds prevail, the evaporation and entrainment feedbacks yield damped modes, indicating that longitudinal variation of the mean surface winds plays an important role in regulation of the MJO intensity in addition to the longitudinal variation of the mean SST. The air–sea interaction over the Indian monsoon region and equatorial Indian Ocean, in cooperation with the instability caused by the local meridional circulation and BL moisture convergence, can support a self-sustained Indian summer monsoon ISO (Liu and Wang 2012b). The monsoon trough over the western North Pacific during late boreal summer favors for a negative air–sea feedback to amplify the local ISO over the western North Pacific (Wang and Zhang 2002; Liu and Wang 2014), which explains why the strongest ISO occurs over the western North Pacific during late boreal summer.

Observed MJO characteristics: setting up theoretical targets

What are the essential phenomenological features of the MJO that theories must explain? This is an indispensable question for establishing and validating MJO theories. Unfortunately, this remains a controversial issue because of the complex nature of the tropical convection associated with MJO. This section is devoted to discuss this issue.

Statistical features of MJO have been well documented, including seasonal variations of intraseasonal variances (Kemball-Cook and Wang 2001), the wavenumber–frequency spectrum and leading Empirical Orthogonal Function modes (Wheeler and Kiladis 1999; Wheeler and Hendon 2004). Statistically, MJO is defined as the spectral components within zonal wavenumbers 1–3 and having periods of 30–80 days in the wavenumber–frequency spectrum of OLR and 850 hPa zonal wind (Waliser 2012). However, to better understand the dynamics of the MJO, it is advantageous to define MJO properties from a dynamic system perspective. In this regard, the essential characteristics of MJO system may embrace the following aspects.

1. MJO is a planetary-scale (dominant zonal wavenumber 1 and 2) circulation system coupled with a large-scale (zonal wavenumber 3–5) convective complex, implying a preferred scale selection exists.
2. MJO moves eastward slowly with a speed of about 5 m/s over the Indo-Pacific warm pool and about 15 m/s over the western hemisphere (Madden and Julian 1972; Knutson and Weickmann 1987), leading to 30–60-day oscillation.
3. The MJO circulation exhibits a coupled Kelvin and Rossby wave structure (Rui and Wang 1990; Hendon and Salby 1994; Adames and Wallace 2014).
4. MJO exhibits a gravest baroclinic circulation structure with a backward-tilted vertical motion and moisture. The BL low-pressure and convergence lead the major convective center (Madden and Julian 1972; Wang 1988b; Hendon and Salby 1994).
5. The MJO system amplifies over the Indo-Pacific warm pool and decays over the cold tongue in the central Pacific and eastern Pacific (Wang and Rui 1990b), implying an instability mechanism exists.

In addition to the aforementioned basic characteristics (1–5), MJO exhibits more complex behaviors that also require theoretical explanation. These include (6) multiscale structure of the convective complex (Nakazawa 1988), implying roles of upscale eddy property transport and multi-cloud effects; (7) strong seasonality (Wang and Rui 1990b), implying impacts of mean states; (8) coupling with ocean mixed layer (Krishnamurti et al. 1988), implying atmosphere–ocean interaction; (9) irregularity in periodicity, propagation, etc., implying roles of stochastic forcing, mid-latitude influences, etc. (10) teleconnection or interaction with mid–high latitude variability.

The three-dimensional structure of the MJO was summarized by the schematic diagram shown in Fig. 1, which can be viewed as an extension of the two-dimensional structure along the equator made by Madden and Julian (Madden and Julian 1972). From a dynamical standpoint, we may define MJO as a tropical, planetary-scale, unstable circulation system (coupled with a multiscale convective complex) that moves eastward slowly (~5 m/s over the war pool ocean) with a rearward-tilted vertical motion and a coupled Kelvin–Rossby wave structure. The rudimentary features of the MJO that requests theoretical explanation include (1) the planetary circulation scale, (2) slow eastward propagation over the warm Indian and western Pacific oceans (about 5 m/s) while fast propagation over the cold eastern Pacific (about 15 m/s), (3) the coupled Kelvin–Rossby wave (horizontal) structure, (4) the backward-tilted baroclinic vertical structure, and (5) the growth (decay) in the warm (cold) oceans. These essential features should be viewed as major targets for theoretical interpretation and validation metrics of any basic MJO theory. The features (6)–(10) are also important but request more complicated or specific models to explain. We consider them as higher order theoretical targets. In this study, we will focus on understanding of the first five basic features of MJO.

A general theoretical model framework for essential dynamics of MJO

The principles for establishment of a theoretical model framework are as follows. (1) The model must be derived from the first principles with reasonable/justifiable assumptions. (2) The model is designed to include only the essential processes to MJO dynamics. (3) The model results are verifiable against observations. (4) The model can elucidate fundamental mechanisms at work. Based on these principles, Wang and Chen (2016) proposed a general model framework for understanding MJO essential dynamics.

Figure 2 illustrates the key elements of large-scale MJO dynamics. The coupled Convection-Kelvin–Rossby wave structure and the phase lead of the BL convergence to convective heating imply that the low-frequency wave and BL dynamics, precipitation heating and their interactions must be the key elements, which also necessarily involve moisture feedback to convective precipitation. The moisture feedback is determined by surface entropy fluxes and the moisture convergence induced by the wave and BL dynamics. The precipitation heat energy comes from the basic state moist static energy that is largely controlled by basic state SST (Wang 1988b; Wang and Li 1994). The model framework shown in Fig. 2 includes all rudimental elements that are considered in the five major existing MJO theories mentioned in "Review of progresses in theoretical understanding" section, thus representing a general model framework for essential dynamics of MJO.

The simplest vertical structure of the model is a 1 and 1/2 layer equatorial beta-plane model, which consists of the first baroclinic mode in the free troposphere and barotropic BL dynamics (Wang 1988b). Detailed derivation of the model equations is given in Hoskins and Wang (2006) and Wang (2012). Briefly, using horizontal velocity scale C_0, length scale $(C_0/\beta)^{1/2}$, timescale $(\beta C_0)^{-1/2}$, geopotential scale C_0^2, moisture scale $d_0\Delta p/g$, where $d_0 = 2p_2C_p\,C_0^2/\Delta pRL_c$, the non-dimensional governing equations are:

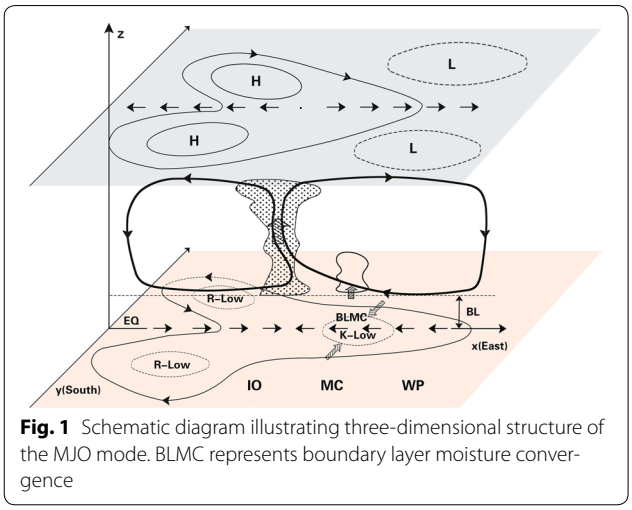

Fig. 1 Schematic diagram illustrating three-dimensional structure of the MJO mode. BLMC represents boundary layer moisture convergence

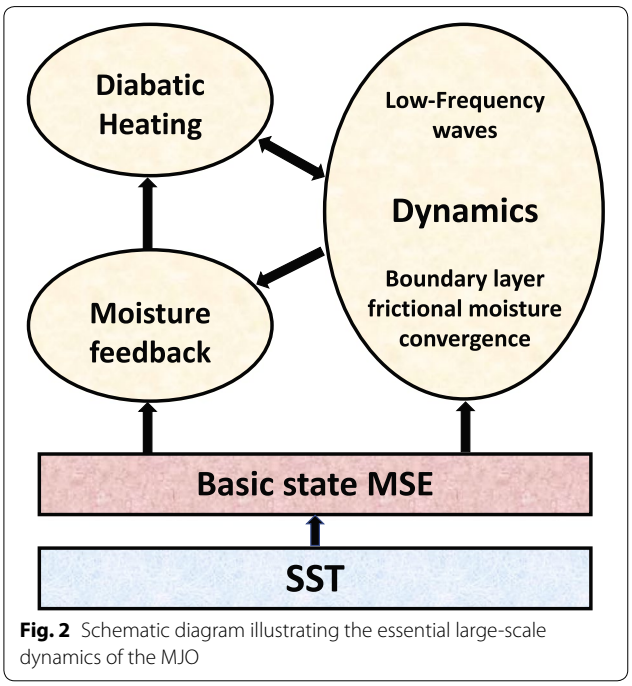

Fig. 2 Schematic diagram illustrating the essential large-scale dynamics of the MJO

$$\frac{\partial u}{\partial t} - yv = -\frac{\partial \Phi}{\partial x} - \epsilon u \tag{1}$$

$$\frac{\partial v}{\partial t} + yu = -\frac{\partial \Phi}{\partial y} - \epsilon v \tag{2}$$

$$\frac{\partial \Phi}{\partial t} + D + dD_b = -(P_r - R) - \mu \Phi \tag{3}$$

$$\frac{\partial q}{\partial t} + \overline{Q}D + \vec{V} \cdot \nabla \overline{Q} + d(\overline{Q}_b D_b + \vec{V}_b \cdot \nabla \overline{Q}_b) = \mathrm{Ev} - P_r \tag{4}$$

$$\frac{\partial u_b}{\partial t} - yv_b = -\frac{\partial \Phi}{\partial x} - E_k u_b \tag{5}$$

$$\frac{\partial v_b}{\partial t} + yu_b = -\frac{\partial \Phi}{\partial y} - E_k v_b \tag{6}$$

Equation (3) is the combined hydrostatic, continuity and thermodynamic equation. Equation (4) is the vertically integrated moisture equation. Equations (5) and (6) are momentum equations for the barotropic BL. u v and Φ represent the free tropospheric low-level zonal wind, meridional wind and geopotential, respectively. $\vec{V}$ and $\vec{V}_b$ denote, respectively, the wind vectors at the low-level free atmosphere and the BL. μ and ϵ are the longwave Newtonian cooling and Rayleigh friction coefficients. q is the column-integrated perturbation moisture from the surface to the tropopause. P_r, R and Ev are precipitation rate, longwave radiation and evaporation, respectively. $\overline{Q}$ and $\overline{Q_b}$ are, respectively, normalized basic state-specific humidity at the lower tropospheric layer and the BL, both are controlled by the underlying SST. For a homogeneous SST, the zonal and meridional moisture advection in Eq. (4) will vanish. D and D_b are the lower tropospheric and BL divergence, respectively. u_b and v_b are BL barotropic winds, and E_k is the friction coefficient in the BL. d is the non-dimensional BL depth. For more details, the reader is referred to Wang and Chen (2016).

The general model framework here can accommodate different convective heating parameterization schemes. Here are examples.

1. Simplified Kuo scheme (Wang and Rui 1990a), in which the moisture tendency is neglected, thus precipitation is balanced by the moisture convergence and surface evaporation:

$$P_r = H\left\{b(\mathrm{Ev} - \overline{Q}D - d\overline{Q}_b D_b)\right\} \tag{7}$$

where b is a precipitation efficiency coefficient. $H(x)$ is a Heaviside function, which represents the positive-only (non-linear) precipitation heating.

2. Simplified convection–moisture feedback sensitivity Bretherton et al. 2004 scheme (Sobel and Maloney 2012; Adames and Kim 2016) in which precipitation heating is proportional to the column-integrated moisture:

$$P_r = \frac{q}{\tau} \tag{8}$$

where τ is the convective timescale.

3. Cloud-radiation feedback scheme (Fuchs and Raymond 2002; Peters and Bretherton 2005) in which the reduction of radiative cooling is proportional to convective heating associated with the precipitation

$$R = -rP_r \tag{9}$$

where r is a coefficient.

4. Simplified B-M scheme (Wang and Chen 2016, Liu and Wang 2016b), in which the moisture is relaxed back to a significant fraction of the saturation value when there is enough moisture for convection: $P_r = \frac{1}{\tau}H(q - \widetilde{q}(T))$ (Frierson et al. 2004), and in the 1 and ½ layer model:

$$P_r = \frac{1}{\tau}H[(q + \alpha\Phi)] \tag{10}$$

where τ is a convective adjustment time.

5. The wave activity ensemble (WAE) scheme (Majda and Stechmann 2009), in which the precipitation tendency is assumed to be proportional to low-level perturbation moisture:

$$\frac{\partial P_r}{\partial t} = Cq_{\mathrm{low}} \tag{11}$$

where C is a constant that is determined by radiative–convective equilibrium state. q_{low} is the low-level moisture (Majda and Stechmann 2009; Stechmann and Majda 2015), which can be approximated to q, since q is mainly contributed by the moisture from the surface to 500-hPa.

6. The triggered convective heating (Yang and Ingersoll 2013) in which convection is assumed to occur in a small area, and is triggered when the pressure anomaly is lower than a threshold:

$$P_r = \begin{cases} \frac{P_{r0}}{\tau A_0}\left[1 - \left(\frac{\Delta t - \tau/2}{\tau/2}\right)^2\right]\left(1 - \frac{L^2}{R^2}\right); \text{when } \phi < \phi_c,\ 0 < \Delta t < \tau, \text{ and } L^2 \le R^2 \\ 0; \text{otherwise,} \end{cases} \tag{12}$$

where $L = (\Delta x^2 + \Delta y^2)^{1/2}$ measures the disturbance from the convective center, Δx and Δy are measured relative to the location where the convection is triggered.

These simplified parameterization schemes shown above all attempt to relate the large-scale convective heating to the large-scale atmospheric variables. The proper representation of convection in terms of the large-scale atmospheric variables affects the ability of a theoretical model to simulate the trio-interaction between convection, moisture, and large-scale circulation, which determines how well a theoretical model can capture the essential features of MJO. Therefore, the validity and limitations of these schemes should be checked against observations.

Relationships between the general MJO model and the existing theoretical models

The governing Eqs. (1–6) for MJO dynamics and the simplified convective parameterization (7–12) have extended the Matsuno (1966)–Gill (1980) model massively by including (a) BL dynamics, (b) moisture conservation, and (c) parameterized interactive convective heating. The major existing theoretical models of MJO can be obtained from this general MJO model by introducing simplified assumptions as discussed below.

1. *The frictionally coupled Kelvin–Rossby wave model* can be obtained using a diagnostic moisture equation and choosing the simplified Kuo scheme, Eq. (7).
2. *The moisture mode theory model* (Sobel and Maloney 2013; Adames and Kim 2016) can be obtained by neglecting the BL dynamics and the tendency terms in the momentum and thermodynamic equations and choosing the simplified convection–moisture sensitivity scheme [Eq. (8)] and cloud-radiation feedback scheme, Eq. (9). It also implemented the effects of the BL frictional convergence and the high-frequency eddy-induced moistening in the moisture Eq. (4), which are both parameterized by the low-level zonal wind anomalies.
3. *The frictionally coupled dynamic moisture mode model* (Wang and Chen 2016, Liu and Wang 2016b) can be obtained by choosing the simplified B-M scheme, Eq. (10), without other simplification.
4. *The MJO skeleton model* (Majda and Stechmann 2009) can be obtained by neglecting the BL dynamics, Rayleigh friction, Newtonian cooling, and spatial variation of $\overline{Q}$, and choosing the WAE precipitation scheme, Eq. (11). The frictional skeleton model (Liu and Wang 2012a) can also be obtained by choosing the WAE precipitation scheme.
5. *The gravity wave interference model* (Yang and Ingersoll 2013) can be obtained by neglecting moisture equation and BL dynamics and choosing the triggered convection scheme, Eq. (12).

Therefore, the major existing theoretical models of MJO are all specific cases of the general MJO model.

The MJO simulated in the MJO trio-interaction model

Hereafter, we focus on the general model with the simplified B-M scheme. The essence of this model lies in a trio-interaction among convective heating, moisture, and equatorial wave-BL dynamics. For this reason, this theory is named as a trio-interaction theory. The trio-interaction mode obtained from this model is essentially a frictionally coupled dynamic moisture mode. There are two fundamental processes that interact with convective heating and support the trio-interaction mode, one is the BL frictional convergence feedback and the other is moisture feedback. Adding additional parametrized terms such as cloud-radiation feedback is trivial.

Figure 3 presents the propagation, horizontal structure, and BL convergence of the simulated MJO-like, trio-interaction mode on an idealized "warm pool" SST configuration (Fig. 3a). The governing equations are solved in an aqua-planet channel between 40°S and 40°N on a spherical coordinate by rewriting Eqs. (1)–(6) to the spherical coordinate. The zonal boundary condition is periodic and the fluxes of mass, momentum, and heat normal to the meridional boundaries vanish. An initial pure Kelvin wave disturbance was placed on the equator and 60°E. The solution is not sensitive to the specified initial disturbance.

With the specified warm pool SST (and basic state moisture distribution), the simulated MJO precipitation anomaly moves eastward from 60°E to 170°E with a speed about 5 m/s comparable to observations (Fig. 3b). Interestingly, the simulated precipitation anomaly amplifies over the warm ocean with the strongest precipitation nearly coinciding with the highest SSTs. The precipitation anomaly decays quickly near the dateline because the westward background SST gradients produce negative moisture advection by MJO easterly and the low SST over cold tongue kills the convection.

The simulated low-level geopotential and wind fields display a coupled convection-Kelvin–Rossby wave pattern (Fig. 3c), the nearly symmetric double cyclone to the west of the precipitation and the low-pressure/easterly anomaly to the east of the precipitation represent the Rossby wave and Kelvin wave components, respectively. This structure resembles closely to the observed structure (Fig. 3d).

The observed (Fig. 3d) and simulated MJO structures (Fig. 3c) bear similarity with the Gill (1980) pattern, but

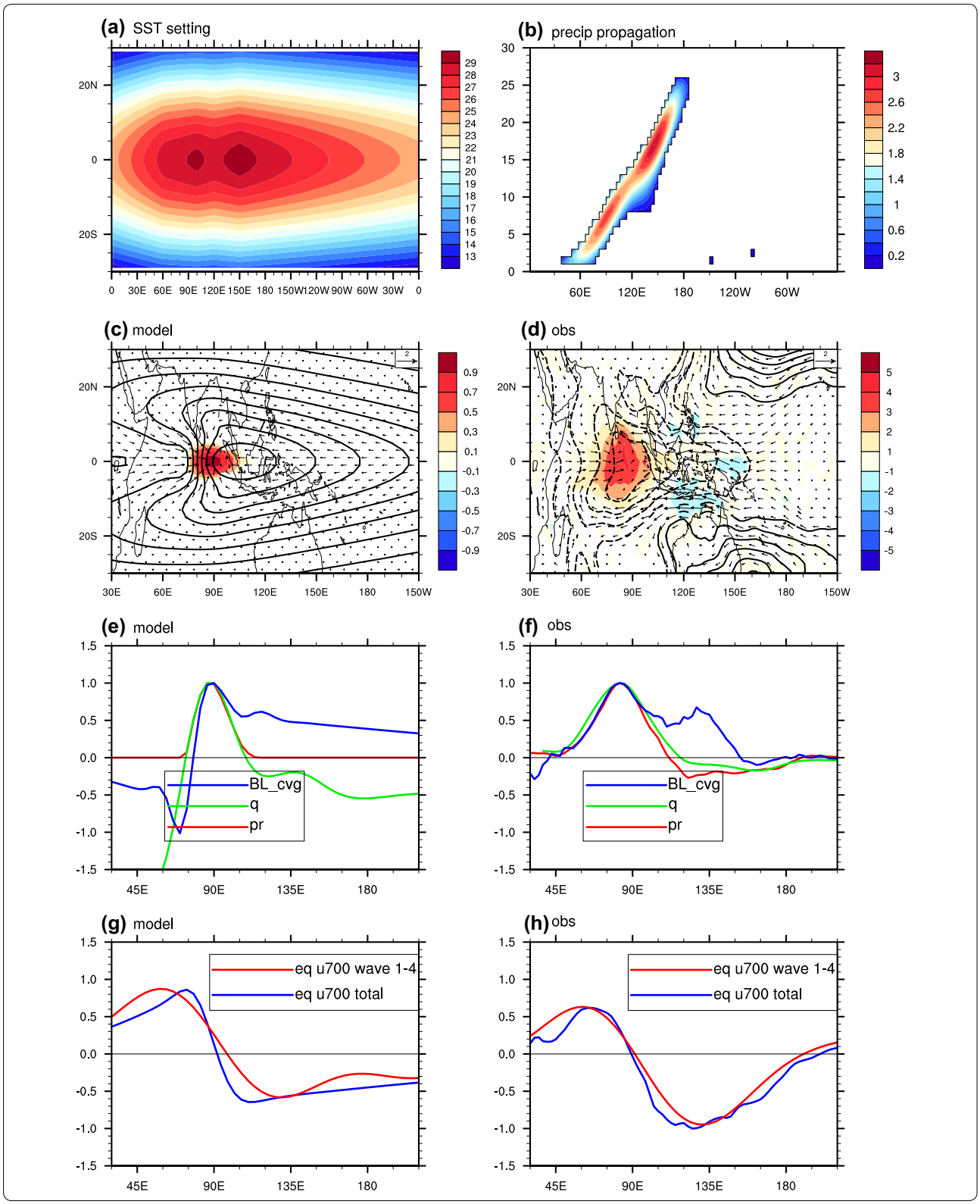
(a) SST setting
20N
0
20S
0 30E 60E 90E 120E 150E 180 150W 120W 90W 60W 30W 0
29 28 27 26 25 24 23 22 21 20 19 18 17 16 15 14 13
(b) precip propagation
30 25 20 15 10 5 0
60E 120E 180 120W 60W
3 2.6 2.2 1.8 1.4 1 0.6 0.2
(c) model
20N
0
20S
30E 60E 90E 120E 150E 180 150W
0.9 0.7 0.5 0.3 0.1 -0.1 -0.3 -0.5 -0.7 -0.9
(d) obs
20N
0
20S
30E 60E 90E 120E 150E 180 150W
5 4 3 2 1 -1 -2 -3 -4 -5
(e) model
1.5 1.0 0.5 0.0 -0.5 -1.0 -1.5
BL_cvg
q
pr
45E 90E 135E 180
(f) obs
1.5 1.0 0.5 0.0 -0.5 -1.0 -1.5
BL_cvg
q
pr
45E 90E 135E 180
(g) model
1.5 1.0 0.5 0.0 -0.5 -1.0 -1.5
eq u700 wave 1-4
eq u700 total
45E 90E 135E 180
(h) obs
1.5 1.0 0.5 0.0 -0.5 -1.0 -1.5
eq u700 wave 1-4
eq u700 total
45E 90E 135E 180

(See figure on previous page.)
Fig. 3 MJO propagation in a varying background SST (°C) simulated in the trio-interaction model with B-M scheme. **a** Idealized Indo-Pacific warm pool SST configuration. **b** Time-longitude diagram of simulated precipitation rate (mm/day) along the equator; **c** simulated normalized low-level (700-hPa) wind (vectors), geopotential height (contour) and the precipitation (shading) at day 7; **d** observed horizontal structures of MJO during winter (NDJFM), namely regressions of 700-hPa wind (m/s, vector), geopotential height (m, contour), as well as precipitation (mm/day, shading) with respect to the precipitation index over the eastern Indian Ocean (averaged over 5°S–5°N; and 70°E–90°E); **e** the simulated equatorial (averaged between 5°S and 5°N) precipitation (*red*), column-integrated moisture (*green*) and BL convergence (*blue*); **f** the same as **e** except for observation; **g** Planetary zonal scale of the MJO mode shown by the low-level equatorial zonal wind (m/s) at day 7 (*blue line*). The *red line* shows the approximate zonal wind made by the first four wavenumbers; **h** the same as **g**, except for the observed MJO zonal scale corresponding to **d**. The observational datasets are ERA-interim atmospheric dataset and TRMM precipitation dataset, with a period from 1998 to 2015

they are not the same. The shape parameter defined by the zonal extent ratio of Kelvin easterly vs. Rossby westerly is 3.0 in Gill pattern but only 2.0 in observed and simulated MJO. The Rossby–Kelvin (R–K) intensity parameter defined by the ratio of the maximum low-level westerly speed $U_{\max}$ vs. the maximum easterly speed $abs(U_{\min})$ averaged over 5°S and 5°N is 2.2 in Gill pattern but only 0.6 and 1.3 in the observed and simulated MJO. The structural differences between the Gill pattern and MJO arise from the nature of the precipitation heating. In the Gill model the heating is specified and the waves are passive responses, while in the MJO structure the heating is interactive with the waves and the waves can feed back to the heating. For this reason, we will describe MJO structure as a coupled Kelvin–Rossby wave packet, avoiding using "Gill pattern".

Figure 3e shows that the simulated BL frictional convergence is located under and to the east of the major convection center, a feature which closely resembles observations (Fig. 3f). The phase shift between the BL convergence and free troposphere upward motion is the 1½ layer model's counterpart of the observed backward-tilted vertical structure in a vertically continuous model. The vertical tilt of moisture field is mainly contributed by the BL frictional convergence to the east of the convective heating.

The planetary (zonal) scale of the simulated MJO low-level zonal winds is further analyzed in Fig. 3g in comparison with observation (Fig. 3h). The zonal circulation is a single wave packet that is primarily made of zonal wavenumber 1–4 with wavenumber 1 having the largest contribution (Wang and Chen 2016). The result here may provide an explanation of the statistical definition of MJO which manifests itself as concentration of energy on wavenumber 1–3 and period of 30–80 days in the frequency–wavenumber spectrum diagram (Wheeler and Hendon 2004; Jiang et al. 2015).

In sum, the trio-interaction model yields an MJO-like mode that captures the five basic characteristics of the observed MJO realistically, producing an equatorial planetary-scale, unstable system moving eastward slowly (~5 m/s) over warm pool with a rearward-tilted, coupled Kelvin–Rossby wave structure.

Mechanisms of MJO offered by the trio-interaction theory

There are a number of fundamental questions regarding the basic mechanisms of the MJO which will be addressed in this section in terms of the trio-interaction theory.

a. Mechanisms for the convective coupling of Kelvin and Rossby waves

Why does MJO exhibit a coupled Kelvin–Rossby wave structure with BL convergence leading convection? To address this question, we use the trio-interaction model with uniform SST of 29.0 °C and compare the results from the models with and without BL dynamics (by setting the BL depth d to zero), respectively.

Figure 4 shows that the same initial dry Kelvin wave low-pressure induces precipitation, which further excites a coupled Kelvin–Rossby system at day 2. With BL dynamics, the trio-interaction mode exhibits a coupled K–R structure (Fig. 4a); however, without the BL dynamics, the Kelvin and Rossby waves are decoupled: the Rossby wave moves westward and the Kelvin wave moves eastward (Fig. 4b). Their propagation speeds are the same as predicted by the equatorial wave theory (Matsuno 1966). Therefore, the moisture feedback in the B-M parameterization could not generate the MJO-like mode. Similarly, without BL dynamics the Kuo scheme and the moisture feedback in the WAE (skeleton model) scheme also cannot hold the Kelvin and Rossby wave together (Fig. 4c, d). It is the BL frictional moisture convergence that is responsible for the coupling among convection, Kelvin and Rossby waves.

How could the BL frictional convergence couple the eastward-propagating Kelvin wave and westward-propagating Rossby waves together with convection and select eastward propagation? Wang and Rui (1990a) showed that the Rossby wave-induced BL convergence exhibits not only off-equatorial maximum coinciding with Rossby wave lows but also an equatorial maximum convergence to the east of the Rossby wave lows; on the other hand, the Kelvin wave-induced BL convergence displays an equatorial maximum that coincides with Kelvin wave low pressure and easterly phase. Therefore, when convective

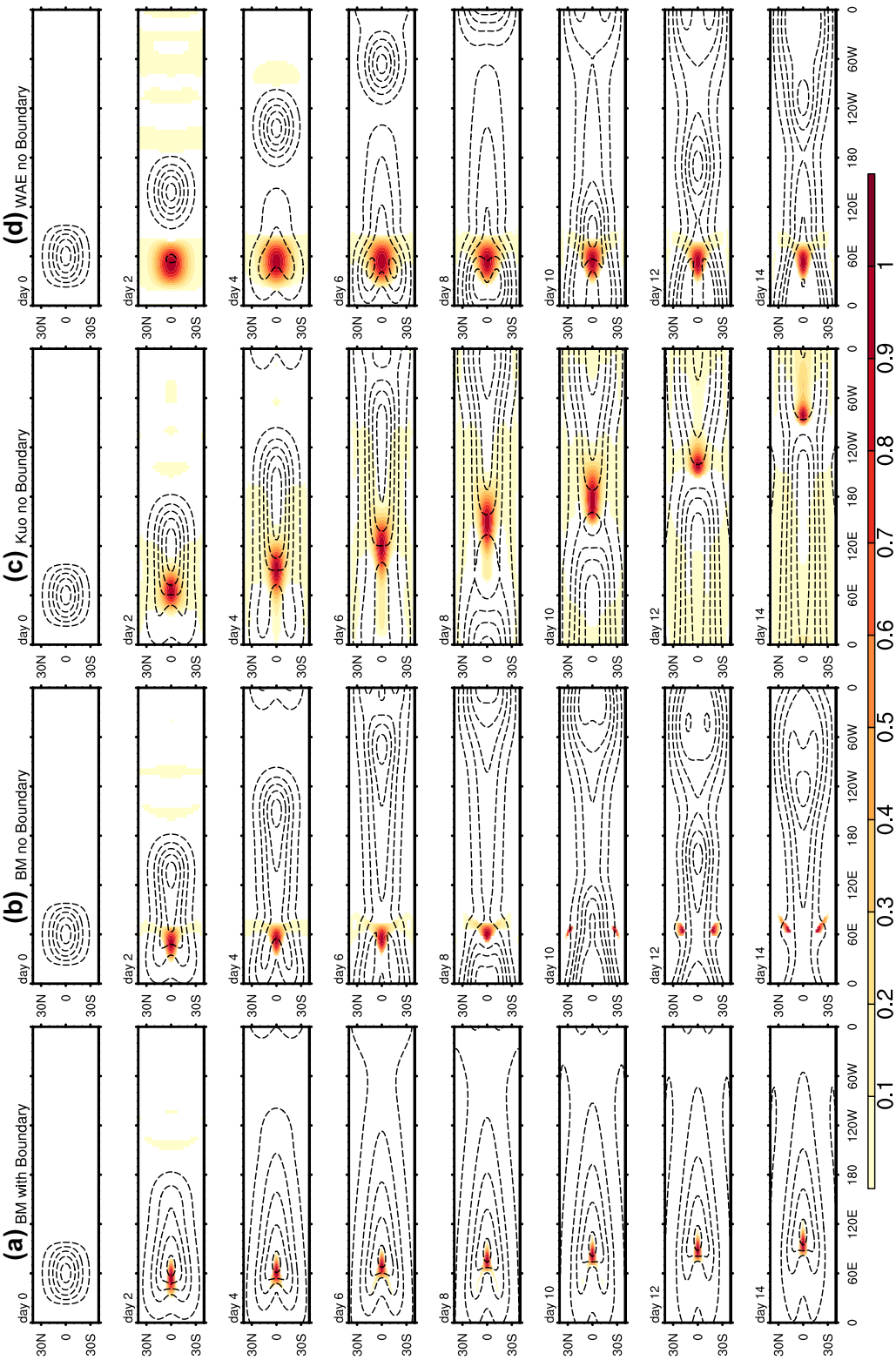

Fig. 4 Comparison of the evolution/propagation of the simulated MJO modes using: **a** B-M scheme with BL dynamics, **b** B-M scheme without BL dynamics, **c** Kuo scheme without BL dynamics, and **d** WAE scheme without BL dynamics. Shown are sequential maps of precipitation rate (*color shading*) and lower troposphere geopotential height (*contours*). All fields are normalized by their respective maxima (absolute values) at each *panel*. The contours start from −0.9 with an interval 0.2. The basic state SST is uniform 29.0 °C

heating excites Rossby wave lows to its west and Kelvin wave low to its east, the Kelvin and Rossby waves would produce a unified BL moisture convergence field that leads (to the east of) the major convective heating (see Fig. 3e). As a result, the frictional organization of convective heating can couple the Kelvin and Rossby waves together with convective heating. The BL moisture convergence can also accumulate moist static energy and increase convective instability to the east of the major convection (Hsu and Li 2012), leading to eastward propagation of the MJO.

b. Mechanisms for slow eastward propagation of MJO

Slow eastward propagation (about 5 m/s) in the warm pool is critical to explain the 30–60-day periodicity of MJO. What controls MJO propagation speed in general? In this subsection, we show that the slow eastward propagation is primarily attributed to (a) warm pool SST, which promotes convective heating that reduces effective static stability, thus reducing the moist equatorial wave speed, (b) the coupling of Kelvin and Rossby waves, and (c) the moisture feedback in the B-M parameterization. To understand the effects of factors (a) and (b), it is convenient to examine the combined dimensional thermodynamic equation and moisture equation without BL and moisture tendency:

$$\frac{\partial \Phi}{\partial t} + C_0^2(1 - b\overline{Q})\nabla \cdot \vec{v} = 0 \tag{13}$$

where C_0 is the dry Kelvin wave or gravity wave speed, which is determined by the dry static stability; b is the precipitation efficiency coefficient (b = 0.88 in this study); the quantity $C_0^2(1 - b\overline{Q})$ represents the effective static stability, which is the reduced static stability due to the precipitation heating. Thus, $C = C_0\sqrt{(1 - b\overline{Q})}$ is the phase speed of convectively coupled Kelvin wave. When SST increases, the $(\overline{Q})$ increases accordingly, thus moist Kelvin wave phase speed decreases.

As shown in Fig. 5, given typical atmospheric static stability parameter, the dry baroclinic Kelvin (gravity) wave speed is 50 m/s. The convectively coupled Kelvin wave (moist-K) speed decreases with increasing SST with a value of 19 m/s for SST = 29 °C. The MJO eastward-propagating speed is further slowed down by the coupling of Kelvin and Rossby waves from 19 to 14.9 m/s when SST = 29 °C with the simplified Kuo scheme (without moisture feedback). This is because the Rossby wave component induced by β-effect tends to move westward. Finally, the moisture feedback in B-M scheme can further substantially slow down the eastward propagation speed to about 5 m/s. The SST dependence of propagation speed is consistent with the observed slow propagation over the warm pool and fast propagation in the cold ocean in the western hemisphere (Knutson et al. 1986).

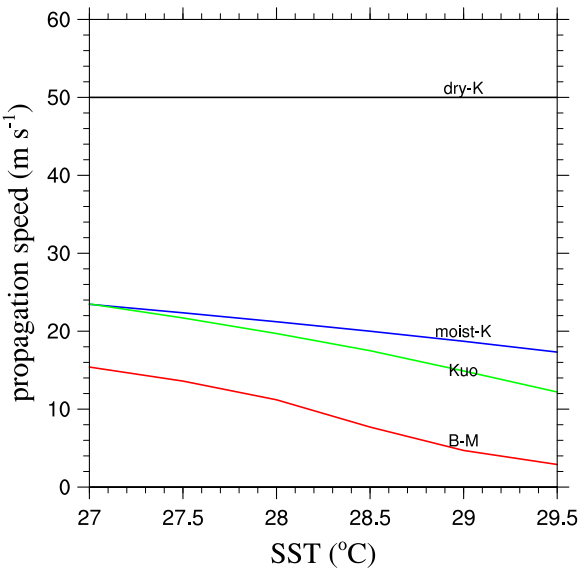

Fig. 5 Eastward propagation speed as function of SST for dry Kelvin wave (Dry-K), moist Kelvin wave (moist-K), coupled Kelvin–Rossby waves in the Kuo simulation (Kuo) and in the B-M simulation (B-M). Adopted from Wang and Chen (2016)

Why does the moisture feedback in the B-M simulation substantially slow down the eastward propagation of the MJO mode? Wang and Chen (2016) has shown that the B-M scheme couples more tightly the convection and Rossby waves, resulting in an enhanced Rossby wave component, which substantially slows down MJO eastward propagation because the Rossby wave component induced by β-effect tends to move westward. The theoretical result here finds support from a previous aquaplanet numerical study, which shows that when Rossby wave component becomes weak, the eastward propagation becomes faster (Kang et al. 2013).

c. Mechanism of amplification and decay of MJO

The MJO instability in the trio-interaction model depends on the basic state SST or basic state moist static energy, which is the ultimate heating energy source for the MJO instability. The non-linear evolution of the simulated MJO mode in Fig. 3b has elucidated why MJO intensifies over the warm pool oceans while decays over the cold ocean. The linear instability analysis of Liu and Wang (2016b) shows that the growth rate of the MJO mode increases as SST increases. Note that the growth rate in the Kuo simulation without moisture feedback is significantly higher than that in the B-M simulation, suggesting the moisture feedback reduces the growth rate.

Why does the moisture feedback in B-M simulation reduce the instability? Energetic analysis provides an answer. The energetic analysis also reveals how MJO

perturbation energy is generated and what characteristic structure a growing MJO mode has. Following Wang and Li (1994), the non-dimensional total energy equation for the free atmosphere could be expressed as:

$$\frac{\partial}{\partial t}\left\langle (u^2+v^2+\Phi^2)/2 \right\rangle = -\langle \Phi H(P_r) \rangle - d\langle \Phi \nabla \cdot \mathbf{V}_b \rangle - \epsilon < u^2+v^2 > -\mu \left\langle \Phi^2 \right\rangle \quad (14)$$

where the angle bracket denotes spatial average over the entire domain. The first term on the right-hand side of Eq. (14) represents the generation of eddy available potential energy (EAPE), which is determined by the negative covariance between precipitation and low-level geopotential height perturbation, and occurs only in the precipitation region; the second to fourth terms represent the energy losses due to BL friction, Rayleigh friction and Newtonian cooling.

Figure 6 shows zonal distribution of EAPE generation along the equator where the EAPE reaches a maximum. In both parameterization schemes, precipitation occurs in the low-level low-pressure regions, so that the covariance between the low-pressure and precipitation heating generates EAPE. The maximum eddy generation rate nearly coincides with precipitation. However, the region of EAPE generation slightly leads the precipitation in both simulations, which is consistent with observations (Johnson et al. 1999). This phase difference also implies that the EAPE generation may contribute to eastward propagation. The model reproduces an important feature that agrees very well with observation, that is, the low sea-level pressure and associated BL convergence leads precipitation region. This can be seen from (a) the low-pressure center and the maximum BL convergence center being located to the east of the precipitation center, and (b) the "integrated" low-pressure and BL convergence to the east of the precipitation center being much stronger than those to the west of the precipitation center.

In addition to the common features in the EAPE generation, there is a difference between the two simulations. As shown in Fig. 6a, the maximum precipitation in Kuo simulation almost coincides with the maximum BL convergence, which means that the frictional moisture convergence can interact directly with precipitation and effectively generate the EAPE. In the B-M simulation, on the other hand, the maximum BL convergence is ahead of the precipitation maxima (Fig. 6b), and the maximum precipitation nearly coincides with the maximum moisture perturbation (not shown here), because the precipitation in the B-M simulation is determined by moisture anomaly, which is a delayed response to frictional moisture convergence, and the release of precipitation heating takes a finite time (the convective adjustment time τ).

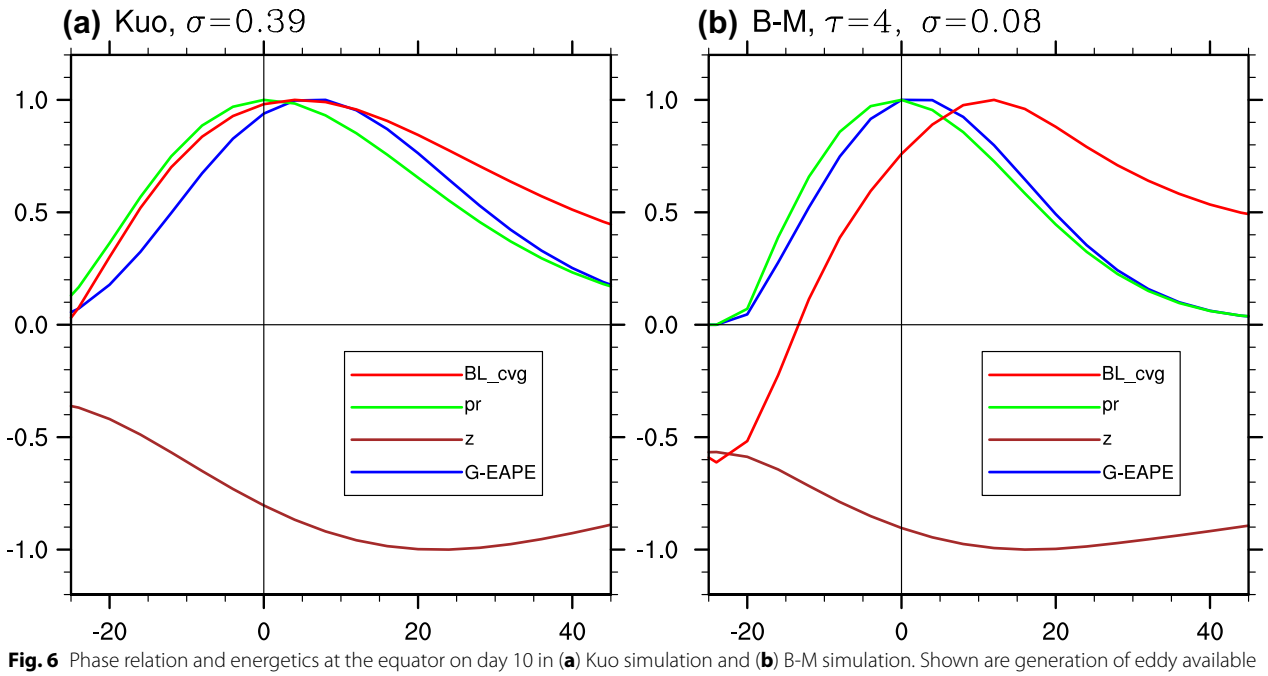

Fig. 6 Phase relation and energetics at the equator on day 10 in (**a**) Kuo simulation and (**b**) B-M simulation. Shown are generation of eddy available potential energy (G-EAPE), geopotential height (z), precipitation (pr), and boundary layer convergence (BL_cvg). All fields are normalized by their respective maxima at each panel. The origin of the zonal *horizontal axis* represents the location of maximum precipitation. σ represents the growth rate (unit 1/day) and τ represents the convective adjustment timescale (unit hour)

Thus, the energy generation rate or the growth rate in the B-M simulation is generally smaller than that in the Kuo simulation. The frictional convergence feedback generates convective available potential energy (CAPE) for the instability; the moisture feedback can reduce the instability by reducing the efficiency of CAPE releasing rate.

Conclusion and discussion

Although notable progress has been made in developing the general circulation models, by far the MJO stays poorly simulated in many models and our prediction skill for MJO remains limited. Lack of adequate understanding of the essential MJO dynamics has resulted in divergent theories.

A general theoretical model for understanding essential dynamics of the MJO is proposed to extend the Matsuno and Gill models by including the trio-interaction among parameterized convective heating, moisture, and the free tropospheric low-frequency equatorial wave dynamics and BL dynamics (Fig. 2). The model accommodates different cumulus parameterization schemes. It is demonstrated that the five types of existing theoretical models are special cases of the general model, including the frictionally coupled Kelvin–Rossby wave model, the moisture mode model, the frictionally coupled dynamic moisture model, the MJO skeleton model, and the gravity wave interference model. The general model allows for considering realistic basic state SST, transient BL, non-linear heating, etc. The general model can also further extend to include other processes that are deemed to have important impacts on MJO's evolution, such as upscale eddy momentum, moisture and heat transfer. The present model can also be extended to a multi-layer model to incorporate multi-layer cloud precipitation effects and explore stratiform cloud–wave interaction and radiation–cloud interaction. These are the future works and are currently underway.

The trio-interaction model with B-M scheme yields a frictionally coupled dynamic moisture mode, which reproduces the following essential characteristics of the observed MJO (Fig. 3): (a) a coupled Kelvin–Rossby wave structure, (b) slow eastward propagation (~5 m/s) over warm pool, (c) planetary (zonal) scale circulation, (d) a vertical structure in which BL moisture convergence leads major convection, and (e) amplification/decay over warm/cold SST regions.

Using trio-interaction model, we demonstrate the frictional convergence feedback provides a mechanism that couples the Kelvin wave and Rossby wave together along with convective heating, and selects eastward propagation. Without frictional convergence feedback, the Kelvin and Rossby waves are decoupled, and there is no growing mode (Fig. 4). Therefore, the frictional convergence feedback acts like an engine that drives the wave dynamic feedback and moisture feedback to generate the unstable dynamic moisture mode.

Interestingly, the model suggests that eastward propagation speed decreases with increasing relative intensity of the Rossby wave component. The moisture feedback in the simplified B-M scheme can enhance the relative intensity of Rossby wave response in the MJO structure, thereby substantially reduce the eastward propagation speed (Fig. 5). The inverse relationship between eastward propagation speed and the relative intensity of the Rossby wave component seems to be consistent with the difference between the models' simulated non-propagating and propagating MJOs (Wang and Chen 2016), but needs to be further verified by observations and model results.

The trio-interaction theory offers answers to three key questions concerning essential dynamics of the MJO: why the MJO possesses a mixed Kelvin–Rossby wave structure; what makes the MJO move eastward slowly (about 5 m/s) in the eastern Hemisphere, resulting in the 30–60-day rhythm, and why MJO amplifies over the warm pool ocean.

The model solutions vary with the model parameters. The most sensitive parameters are the BL Ekman number E_k and the convective adjustment time τ in the B-M scheme. An enhanced BL convergence would enhance frictional moisture feedback, resulting in stronger instability and enhanced Rossby wave component that slows down eastward propagation. A longer adjustment time τ means slower atmospheric adjustment toward the quasi-equilibrium reference state, thus the precipitation intensity weakens, leading to weaker instability.

The results of this study suggest that MJO propagation and instability are sensitive to cumulus parameterization schemes because different schemes may produce different structures of the MJO and propagation speeds, and the EAPE generation is related to the horizontal structures. The observed MJO structure consists of Kelvin wave and Rossby wave components but it is not the same as Gill pattern because the heating in Gill model is specified whereas the heating in MJO interacts with dynamics and moisture. Even within the chosen B-M scheme, the instability and propagation speed depend on sensitive parameters such as the convective adjustment time τ. This may explain why a variety of MJO behaviors have been produced in GCMs and why tuning parameters or change of cumulus parameterization can effectively improve the MJO simulation.

In both observation (Benedict and Randall 2007; Hsu and Li 2012) and model simulation (Jiang and al 2015), the BL frictional convergence has been found to be important for the eastward propagation of the MJO by strongly coupling with the shallow/congestus clouds, resulting in a vertically rearward-tilted structure of the MJO. To validate the critical role of the BL moisture convergence in the trio-interaction theory and to diagnose

numerical models' problems, we suggest focusing on the zonal structural asymmetry in the lower troposphere generated by the BL moisture feedback, including the phase leading of the BL moisture convergence to major convection (by about 4–5 days) and the associated lower troposphere moistening (increase in equivalent potential temperature), destabilization (increase of the convective instability), the 700 hPa diabatic heating and the generation of MJO available potential energy. In the models with good MJO simulation, the BL convergence can enhance congestus cloud heating and upward transport of moisture that further feeds back to BL moisture convergence. This positive feedback could amplify the effects of frictional convergence feedback. In the models with poor MJO simulation, the BL convergence is very weak to the east of MJO convective center, while the associated shallow convective heating as well as the vertically tilted structure disappears (Jiang and al 2015). This implies that MJO simulation may be sensitive to shallow and congestus cumulus parameterization schemes and the BL turbulence parameterization in GCMs. While the BL frictional convergence always exists in GCMs to various degrees, the ways by which BL convergence interacts with shallow and congestus clouds in different GCMs may differ and this interaction could significantly affect the frictional convergence feedback and thus the MJO behavior. This interactive process should be represented correctly in the numerical modeling of MJO with GCMs, including the lower tropospheric convective mixing and low cloud feedback.

Authors' contributions

BW wrote the major parts of the manuscript. FL supplemented some parts of the manuscript and commented on the manuscript. GC supplemented some parts of the manuscript and provided all drawings as well as commented on the manuscript. All authors read and approved the final manuscript.

Author details

[1] Earth System Modeling Center, Nanjing University of Information Science and Technology, Nanjing, China. [2] Department of Atmospheric Sciences and Atmosphere-Ocean Research Center, University of Hawaii at Manoa, Honolulu, HI 96822, USA.

Acknowledgements

This work is supported by the NSF award #AGS-1540783 and the Atmosphere–Ocean Research Center sponsored by the Nanjing University of Information Science and Technology and University of Hawaii. This is the SEOST publication 9875, IPRC publication 1229 and ESMC publication 132.

Competing interests

The authors declare that they have no competing interests.

Received: 15 September 2016 Accepted: 29 November 2016
Published online: 09 December 2016

References

Adames ÁF, Kim D (2016) The MJO as a dispersive, convectively coupled moisture wave: theory and observations. J Atmos Sci 73:913–941

Adames ÁF, Wallace JM (2014) Three-dimensional structure and evolution of the vertical velocity and divergence fields in the MJO. J Atmos Sci 71:4661–4681

Andersen JA, Kuang Z (2012) Moist static energy budget of MJO-like disturbances in the atmosphere of a zonally symmetric aquaplanet. J Clim 25:2782–2804

Benedict JJ, Randall DA (2007) Observed characteristics of the MJO relative to maximum rainfall. J Atmos Sci 64:2332–2354

Biello JA, Majda AJ (2005) A new multiscale model for the Madden–Julian oscillation. J Atmos Sci 62:1694–1721

Boos WR, Kuang Z (2010) Mechanisms of poleward propagating, intraseasonal convective anomalies in cloud system-resolving models. J Atmos Sci 67:3673–3691

Bretherton CS, Peters ME, Back LE (2004) Relationships between water vapor path and precipitation over the tropical oceans. J Clim 17:1517–1528

Chen G, Wang B (2016) Reexamination of the wave activity envelope convective scheme in theoretical modeling of MJO. J Clim. doi:10.1175/JCLI-D-16-0325.1

DeMott CA, Stan C, Randall DA (2013) Northward propagation mechanisms of the boreal summer intraseasonal oscillation in the ERA-Interim and SP-CCSM. J Clim 26:1973–1992

Drbohlav HKL, Wang B (2005) Mechanism of the northward-propagating intraseasonal oscillation: insights from a zonally symmetric model*. J Clim 18:952–972

Emanuel KA (1987) An air-sea interaction model of intraseasonal oscillations in the tropics. J Atmos Sci 44:2324–2340

Flatau M, Flatau PJ, Phoebus P, Niiler PP (1997) The feedback between equatorial convection and local radiative and evaporative processes: the implications for intraseasonal oscillations. J Atmos Sci 54:2373–2386

Frierson DM, Majda AJ, Pauluis OM (2004) Large scale dynamics of precipitation fronts in the tropical atmosphere: a novel relaxation limit. Commun Math Sci 2:591–626

Fu X, Wang B (2004) The Boreal-Summer intraseasonal oscillations simulated in a hybrid coupled atmosphere–ocean model*. Mon Weather Rev. 132:2628–2649

Fu X, Wang B (2009) Critical roles of the stratiform rainfall in sustaining the Madden–Julian oscillation: GCM experiments. J Clim 22:3939–3959

Fuchs Ž, Raymond DJ (2002) Large-scale modes of a nonrotating atmosphere with water vapor and cloud-radiation feedbacks. J Atmos Sci 59:1669–1679

Gill AE (1980) Some simple solutions for heat-induced tropical circulation. Q J R Meteorol Soc. 106:447–462

Grabowski WW, Moncrieff M (2004) Moisture–convection feedback in the tropics. Q J R Meteorol Soc. 130:3081–3104

Gyoswami B, Shukla J (1984) Quasi-periodic oscillations in a symmetric general circulation model. J Atmos Sci 41:20–37

Hendon HH, Salby ML (1994) The life cycle of the Madden–Julian oscillation. J Atmos Sci 51:2225–2237

Hoskins B, Wang B (2006) Large-scale atmospheric dynamics. The Asian Monsoon. Springer, Berlin, pp 357–415

Hsu P-C, Li T (2012) Role of the boundary layer moisture asymmetry in causing the eastward propagation of the Madden–Julian oscillation*. J Clim 25:4914–4931

Jiang X et al (2015) Vertical structure and physical processes of the Madden–Julian oscillation: exploring key model physics in climate simulations. J Geophys Res Atmos 120:4718–4748

Jiang X, Li T, Wang B (2004) Structures and Mechanisms of the northward propagating boreal summer intraseasonal oscillation*. J Clim 17:1022–1039

Johnson RH, Rickenbach TM, Rutledge SA, Ciesielski PE, Schubert WH (1999) Trimodal characteristics of tropical convection. J Clim 12:2397–2418

Kang IS, Kim D, Kug JS (2010) Mechanism for northward propagation of boreal summer intraseasonal oscillation: convective momentum transport. Geophys Res Lett 37:24804

Kang IS, Liu F, Ahn MS, Yang YM, Wang B (2013) The role of SST structure in convectively coupled Kelvin–Rossby waves and its implications for MJO formation. J Clim 26:5915–5930

Kemball-Cook S, Wang B (2001) Equatorial waves and air-sea interaction in the boreal summer intraseasonal oscillation. J Clim 14:2923–2942

Khouider B, Majda AJ (2006) A Simple multicloud parameterization for convectively coupled tropical waves. Part I: linear analysis. J Atmos Sci 63:1308–1323

Khouider B, Majda AJ (2007) A simple multicloud parameterization for convectively coupled tropical waves. Part II: nonlinear simulations. J Atmos Sci 64:381–400
Kikuchi K, Takayabu YN (2004) The development of organized convection associated with the MJO during TOGA COARE IOP: trimodal characteristics. Geophys Res Lett 31:L10101. doi:10.1029/2004GL019601
Kiladis GN, Wheeler MC, Haertel PT, Straub KH, Roundy PE (2009) Convectively coupled equatorial waves. Rev Geophys 47:2003
Kim D, Kug J-S, Sobel AH (2014) Propagating versus nonpropagating Madden–Julian oscillation events. J Clim 27:111–125
Knutson TR, Weickmann KM (1987) 30–60 day atmospheric oscillations: composite life cycles of convection and circulation anomalies. Mon Weather Rev 115:1407–1436
Knutson TR, Weickmann KM, Kutzbach JE (1986) Global-scale intraseasonal oscillations of outgoing longwave radiation and 250 mb zonal wind during northern hemisphere summer. Mon Weather Rev. 114:605–623
Krishnamurti TN, Oosterhof DK, Mehta AV (1988) Air–sea interaction on the time scale of 30 to 50 days. J Atmos Sci 45:1304–1322
Kuang Z (2008) A moisture-stratiform instability for convectively coupled waves. J Atmos Sci 65:834–854
Lau K, Peng L (1987) Origin of low-frequency (intraseasonal) oscillations in the tropical atmosphere. Part I: basic theory. J Atmos Sci 44:950–972
Lee SS, Wang B, Waliser DE, Neena JM, Lee JY (2015) Predictability and prediction skill of the boreal summer intraseasonal oscillation in the intraseasonal variability hindcast experiment. Clim Dyn 45:2123–2135
Li T, Zhou C (2009) Planetary scale selection of the Madden–Julian oscillation*. J Atmos Sci 66:2429–2443
Lin J, Mapes B, Zhang M, Newman M (2004) Stratiform precipitation, vertical heating profiles, and the Madden–Julian oscillation. J Atmos Sci 61:296–309
Liu F, Wang B (2012a) A frictional skeleton model for the Madden–Julian oscillation. J Atmos Sci 69:2749–2758
Liu F, Wang B (2012b) A conceptual model for self-sustained active-break Indian summer monsoon. Geophys Res Lett 39:L20814
Liu F, Wang B (2012c) A model for the interaction between 2-day waves and moist kelvin waves. J Atmos Sci 69:611–625
Liu F, Wang B (2013a) An air–sea coupled skeleton model for the Madden–Julian oscillation. J Atmos Sci 70:3147–3156
Liu F, Wang B (2013b) Impacts of upscale heat and momentum transfer by moist Kelvin waves on the Madden–Julian oscillation: a theoretical model study. Clim Dynam 40:213–224
Liu F, Wang B (2014) A mechanism for explaining the maximum intraseasonal oscillation center over the western north pacific*. J Clim 27:958–968
Liu F, Wang B (2016a) Role of horizontal advection of seasonal-mean moisture in the Madden–Julian oscillation: a theoretical model analysis. J Clim. doi:10.1175/JCLI-D-1116-0078.1171
Liu F, Wang B (2016b) Effects of moisture feedback in a frictional coupled Kelvin–Rossby wave model and implication in the Madden–Julian oscillation dynamics. Clim Dynam. doi:10.1007/s00382-00016-03090-y
Liu F, Huang G, Feng L (2012) Critical roles of convective momentum transfer in sustaining the multi-scale Madden–Julian oscillation. Theor Appl Climatol 108:471–477
Liu F, Wang B, Kang I-S (2015) Roles of barotropic convective momentum transport in the intraseasonal oscillation. J Clim 28:4908–4920
Madden RA, Julian PR (1971) Detection of a 40–50 day oscillation in the zonal wind in the tropical pacific. J Atmos Sci 28:702–708
Madden RA, Julian PR (1972) Description of global-scale circulation cells in the tropics with a 40–50 day period. J Atmos Sci 29:1109–1123
Majda AJ, Biello JA (2004) A multiscale model for tropical intraseasonal oscillations. Proc Natl Acad Sci USA 101:4736–4741
Majda AJ, Stechmann SN (2009) The skeleton of tropical intraseasonal oscillations. Proc Natl Acad Sci 106:8417–8422
Majda AJ, Stechmann SN, Khouider B (2007) Madden–Julian Oscillation analog and intraseasonal variability in a multicloud model above the equator. Proc Natl Acad Sci USA 104:9919–9924
Maloney ED (2009) The moist static energy budget of a composite tropical intraseasonal oscillation in a climate model. J Clim 22:711–729
Maloney ED, Sobel AH, Hannah WM (2010) Intraseasonal variability in an aquaplanet general circulation model. J Adv Model Earth Syst 2:1–14
Mapes BE (2000) Convective inhibition, subgrid-scale triggering energy, and stratiform instability in a toy tropical wave model. J Atmos Sci 57:1515–1535
Mapes B, Tulich S, Lin J, Zuidema P (2006) The mesoscale convection life cycle: building block or prototype for large-scale tropical waves? Dynam Atmos Oceans 42:3–29
Matsuno T (1966) Quasi-geostrophic motions in the equatorial area. J Meteor Soc Jpn 44:25–43
Moskowitz BM, Bretherton CS (2000) An analysis of frictional feedback on a moist Equatorial Kelvin mode. J Atmos Sci 57:2188–2206
Nakazawa T (1988) Tropical super clusters within intraseasonal variations over the western Pacific. J Meteor Soc Jpn 66:823–839
Neelin JD, Held IM, Cook KH (1987) Evaporation-wind feedback and low-frequency variability in the tropical atmosphere. J Atmos Sci 44:2341–2348
Neena JM, Lee JY, Waliser D, Wang B, Jiang X (2014) Predictability of the Madden–Julian oscillation in the Intraseasonal variability hindcast experiment (ISVHE). J Clim 27:4531–4543
Peters ME, Bretherton CS (2005) A simplified model of the walker circulation with an interactive ocean mixed layer and cloud-radiative feedbacks. J Clim 18:4216–4234
Pritchard MS, Bretherton CS (2014) Causal evidence that rotational moisture advection is critical to the superparameterized Madden–Julian oscillation. J Atmos Sci 71:800–815
Pritchard MS, Yang D (2016) Response of the superparameterized Madden–Julian oscillation to extreme climate and basic-state variation challenges a moisture mode view. J Clim 29:4995–5008
Rui H, Wang B (1990) Development characteristics and dynamic structure of tropical intraseasonal convection anomalies. J Atmos Sci 47:357–379
Seo K-H, Wang W (2010) The Madden–Julian oscillation simulated in the NCEP climate forecast system model: the importance of stratiform heating. J Clim 23:4770–4793
Sobel A, Maloney E (2012) An idealized semi-empirical framework for modeling the Madden–Julian oscillation. J Atmos Sci 69:1691–1705
Sobel A, Maloney E (2013) Moisture modes and the eastward propagation of the MJO. J Atmos Sci 70:187–192
Stechmann SN, Majda AJ (2015) Identifying the skeleton of the Madden–Julian oscillation in observational data. Mon Weather Rev 143:395–416
Thual S, Majda AJ, Stechmann SN (2014) A Stochastic skeleton model for the MJO. J Atmos Sci 71:697–715
Vitart F (2014) Evolution of ECMWF sub-seasonal forecast skill scores. Q J R Meteorol Soc 140:1889–1899
Waliser DE (2012) The "year" of tropical convection (May 2008–April 2010): climate variability and weather highlights. Bull Am Meteorol Soc 93:1189–1218
Wang B (1988a) Comments on "An air-sea interaction model of intraseasonal oscillation in the tropics". J Atmos Sci 45:3521–3525
Wang B (1988b) Dynamics of tropical low-frequency waves: an analysis of the moist Kelvin wave. J Atmos Sci 45:2051–2065
Wang B (2012) Theory. In: Lau WKM, Waliser DE (eds) Intraseasonal variability in the atmosphere–ocean climate system, 2nd edn. Springer, Berlin, pp 335–398
Wang B, Chen J (1989) On the zonal-scale selection and vertical structure of equatorial intraseasonal waves †. Q J R Meteorol Soc 115:1301–1323
Wang B, Chen G (2016) A general theoretical framework for understanding essential dynamics of Madden–Julian oscillation. Clim Dyn, accepted
Wang B, Li T (1994) Convective interaction with boundary-layer dynamics in the development of a tropical intraseasonal system. J Atmos Sci 51:1386–1400
Wang B, Liu F (2011) A model for scale interaction in the Madden–Julian oscillation. J Atmos Sci 68:2524–2536
Wang B, Moon JY (2016) Sub-seasonal prediction of extreme weather events, in "bridging science and policy implication for managing climate extremes: linking science and policy implication". In: Chung CS, Wang B (eds). World Scientific Series of Asia-Pacific Weather and Climate Press. Revised
Wang B, Rui H (1990a) Dynamics of the coupled moist Kelvin–Rossby wave on an equatorial β-plane. J Atmos Sci 47:397–413
Wang B, Rui H (1990b) Synoptic climatology of transient tropical intraseasonal convection anomalies: 1975–1985. Meteorol Atmos Phys 44:43–61
Wang B, Xie X (1997) A Model for the boreal summer intraseasonal oscillation. J Atmos Sci 54:72–86

Wang B, Xie X (1998) Coupled modes of the warm pool climate system. Part I: the role of air–sea interaction in maintaining Madden–Julian oscillation. J Clim 11:2116–2135
Wang B, Zhang Q (2002) Pacific-East Asian teleconnection. Part II: how the Philippine Sea anomalous anticyclone is established during El Niño development*. J Clim 15:3252–3265
Webster PJ, Holton JR (1982) Cross-equatorial response to middle-latitude forcing in a zonally varying basic state. J Atmos Sci 39:722–733
Wheeler MC, Hendon HH (2004) An all-season real-time multivariate MJO index: development of an Index for monitoring and prediction. Mon Weather Rev 132:1917–1932
Wheeler M, Kiladis GN (1999) Convectively coupled equatorial waves: analysis of clouds and temperature in the wavenumber-frequency domain. J Atmos Sci 56:374–399
Woolnough S, Slingo J, Hoskins B (2001) The organization of tropical convection by intraseasonal sea surface temperature anomalies. Q J R Meteorol Soc 127:887–907
Xiang B, Zhao M, Jiang X, Lin S-J, Li T, Fu X, Vecchi G (2015) The 3–4-week MJO prediction skill in a GFDL coupled model. J Clim 28:5351–5364
Yang D, Ingersoll AP (2011) Testing the hypothesis that the MJO is a mixed Rossby-Gravity wave packet. J Atmos Sci 68:226–239
Yang D, Ingersoll AP (2013) Triggered convection, gravity waves, and the MJO: a shallow-water model. J Atmos Sci 70:2476–2486
Yang D, Ingersoll AP (2014) A theory of the MJO horizontal scale. Geophys Res Lett 41:1059–1064
Zhang C (2013) Madden–Julian oscillation: bridging Weather and Climate. Bull Am Meteorol Soc 94:1849–1870